

ENHANCEMENT OF ORIENTATED GRAIN GROWTH AND PHOTO RESPONSE OF ZnO THIN FILM BY SILAR

D. THOMAS^{a, b*}, S. C. VATTAPPALAM^b, S. MATHEW^b, S. AUGUSTINE^b

^aResearch and Development Centre, Bharathiar University, Coimbatore, India - 641046

^bPostgraduate and Research Department of Physics, St. Thomas College, Palai, Kerala - 686 574, India

ZnO thin films were prepared by Successive Ionic Layer Adsorption Reaction (SILAR) method. The variations in the oriented grain growth in the thin films annealed in oxygen, air, argon, nitrogen atmospheres and samples doped with aluminium annealed in air were studied. Oriented grain growth was measured by comparing the peak intensities of the XRD pattern. Oriented grain growth increases in the order of samples annealed in atmospheres of oxygen, air, argon, nitrogen and aluminium doped. From the SEM micrographs it is found that as the oriented grain growth increases the needle like structure disappears and flowered structure becomes prominent. When the oriented grain growth increases, crystallinity of the thin film improves, photo current and dark current increases resistance and band gap decreases. ZnO thin films having good (002) orientation is a prerequisite for the fabrication of devices like UV diode lasers, acoustic-optic devices etc. The results also indicate that the ZnO is beneficial to solar cells and photodynamic therapy technology. From energy dispersive X-ray analysis, it is inferred that oxygen vacancy creation is responsible for the enhanced oriented grain growth in ZnO thin films when samples are annealed in atmospheres of argon, nitrogen and aluminium doped.

(Received May 7, 2014; Accepted July 17, 2014)

Keywords: ZnO thin film, SILAR method, Oriented grain growth, Annealing, Al-doping.

1. Introduction

Nearly half a century, ZnO thin films has been an active area of research. ZnO with wurtzite structure [1] is an n-type semiconductor with direct band gap of 3.37eV [2, 3] and high electronic mobility. The wide and direct band gap semiconductor, nanostructured ZnO thin films have attracted attention in optoelectronic devices [4]. The transparent conductive oxide (TCO) electrodes using Al-doped ZnO have used as a powerful candidate material for ITO transparent electrodes [5]. ZnO thin films can be tailored to attain high electrical conductivity, high infrared reflectance and high visible transmittance, by applying different techniques [6, 7, 8, 9]. Different methods have been applied to obtain ZnO thin films. These include magnetron sputtering [7], chemical bath deposition [10], sol-gel [11], spray pyrolysis [12] etc. Chemical deposition techniques are low cost processes and can be easily scaled up for industrial application. Among the thin films deposition techniques, double dip technique from aqueous solutions is the simplest and the most economical one. Double dip method, otherwise called SILAR method, (Successive Immersion Layer Adsorption Reaction) [6, 13, 14] offers the doping of host ions with impurities on different kinds, shapes and sizes on substrates with ease. Zinc oxide crystallites with preferential grain growth along c-axis are suitable for applications such as UV diode lasers acousto-optic devices [4] etc. There are reports of enhanced oriented grain growth in ZnO thin

*Corresponding author: deepuskariankal@gmail.com

films by doping and annealing. The controllable n-type doping can easily achieved by substituting Zn with group-III elements such as Al [6, 7]. The band gap of the samples can be tuned from 3.37 to 3.2 eV if it is doped with group III metal ions. It is reported that oriented grain growth of the samples was significantly enhanced due to Al doping [6], by annealing the samples in argon atmosphere [15, 16] and nitrogen atmosphere [4, 17]. Even though, there are reports on enhancement of oriented grain growth in ZnO by annealing and doping, a study on the variation of oriented grain growth in ZnO thin films under the above experimental conditions and its possible mechanism is not yet carried out extensively.

In course of the present investigations, the variations in the oriented grain growth in ZnO thin films annealed in oxygen, air, argon, nitrogen atmospheres and samples doped with aluminium are studied. A possible mechanism for the oriented grain growth is also investigated.

2. Experimental

ZnO thin films were prepared by Successive Ionic Layer Adsorption Reaction (SILAR) method, in which, the ZnO thin film was coated on a glass substrate (26 × 76 mm) by alternately dipping it in a sodium zincate bath at room temperature and then in hot water maintained at 90-95°C. Rostov et al. [18] had already used this method for preparing Cu_2O thin films and R. Chandramohan et al. for ZnO thin films [6]. Sodium zincate bath was prepared by using 1 molar zinc sulphate [$ZnSO_4 \cdot 7H_2O$] and 2 molar sodium hydroxide [NaOH]. Aluminium doping was done by adding anhydrous aluminium chloride [$AlCl_3$] in sodium zincate bath. Before deposition, the glass substrates were cleaned in chromic acid followed by cleaning with acetone. The well-cleaned substrates were immersed in the chemical bath for 10 second followed by immersion in hot water for an equal duration and the process was repeated 100 times. These samples were annealed at 450°C for half an hour in oxygen, air, argon, and nitrogen atmospheres. The flow rate of the gases was 2 liters/minute. The doped sample was also annealed at 450°C for half an hour in air. The structural analysis of the thin films was done by X-ray diffraction (XRD) and surface morphology by scanning electron microscopy (SEM). X-ray diffraction was performed on Bruker AXS-8 using $CuK\alpha$ radiation and SEM micrographs were taken by using JEOL -JSM6490. Chemical elemental stoichiometry was examined based on energy dispersive X-ray analysis (EDAX) linked with SEM unit. The electrical resistance of ZnO thin film at room temperature was measured by Keithley 2100 Digital Multimeter. The optical absorbance was measured in the wavelength range of 190-1100 nm by means of a UV-VIS spectrophotometer. The photoconductivity of the samples were studied by Keithley 6485 picometer. Oriented grain growth of the samples was measured by using an orientation index (O.I.), which is the ratio of the intensities of (002) reflection ($2\theta = 34^\circ$) to (101) reflection ($2\theta = 36^\circ$) in the XRD.

$$O.I = I_{002}/I_{101}$$

3 Results and discussion

3.1 Structural characterization and Morphological studies

XRD patterns of ZnO thin films annealed in oxygen, air, argon and nitrogen atmospheres are depicted in figs. 1 (a-d) and doped sample is depicted in figs. 2. It is seen from figures that the (002) peak appears with maximum intensity at $2\theta = 34^\circ$. The other peaks at 31° and 36° can be associated with (100), (101) reflections of ZnO, as is expected for wurtzite hexagonal structure (JCPDS no.36-1451). It is particularly observed that the intensity of the (002) peak is enhanced with the annealing in air, argon atmosphere, nitrogen atmosphere and doping with aluminium. The (002) diffraction peak exhibited a higher intensity, indicating that the grain growth is along (002) plane. Figures 3 (a) and 3 (b) show the SEM micrographs of the pure and aluminium doped samples annealed in air. From the figs. 1(a-d) and from table- 1, it is clear that oriented grain growth in the samples increases in the order of samples annealed in atmospheres of oxygen, air,

argon, nitrogen and aluminium doped. The needle like and flowered structure of ZnO is evident from the SEM micrograph of the pure sample (fig.3 (a)). But when the samples annealed in atmospheres of argon, nitrogen and doped with aluminium, the needle like structure disappears and flowered structure becomes prominent. This is due to the expansion of grain size by the annealing of the samples in atmospheres of argon, nitrogen and doping with aluminium. The average grain size of the ZnO crystals in the films was calculated by using Scherrers formula: $D = 0.9\lambda/\beta \cos\theta$, where D is the grain size, λ - the wavelength of X-ray used, β - the FWHM(full width half maximum) and θ - Bragg angle. From the studies, the grain size of the samples is found to be in the range 18- 33nm (Table-1). The larger values of D indicate better crystallization of the films. As the values of D increases, the orientation index is found to be increased. Increase in orientation index indicates the increases in the crystallinity in ZnO thin films. Thus the prepared films having good crystallinity with preferential (002) orientation is a prerequisite for the fabrication of devices like UV diode lasers, acoustic-optic devices etc. [19].

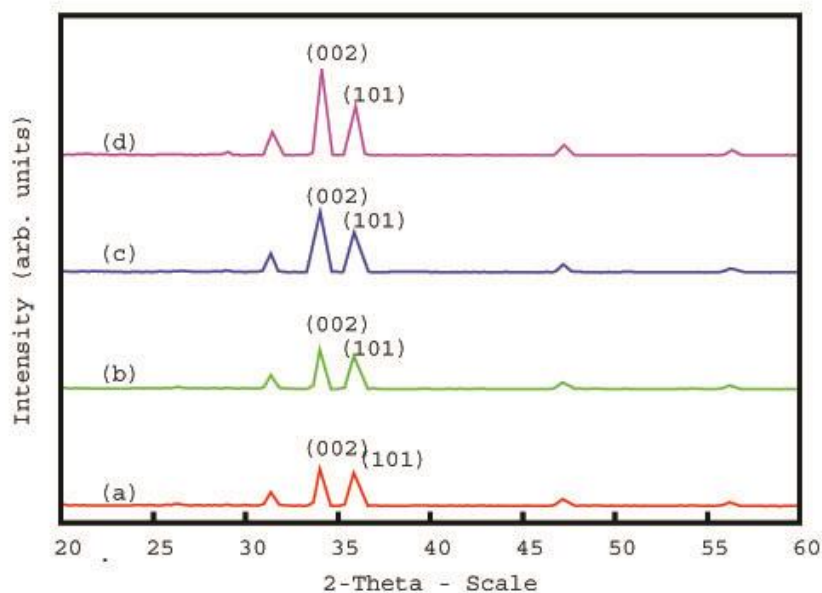


Fig. 1. XRD patterns of the samples annealed in (a) oxygen atmosphere (b) air (c) argon atmosphere (d) nitrogen atmosphere.

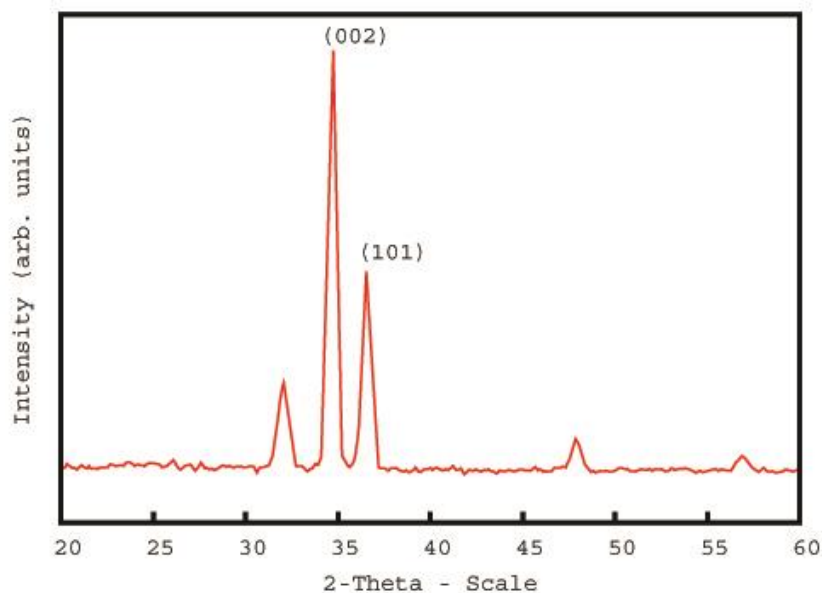


Fig. 2. XRD pattern of the sample doped with aluminium

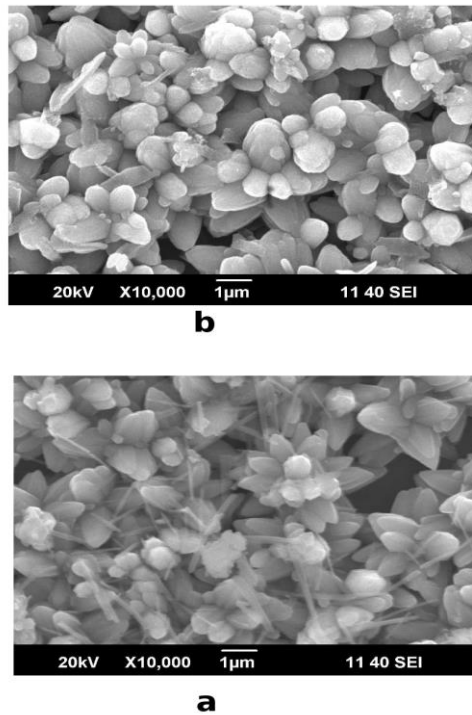


Fig. 3. SEM micrographs of the samples annealed in (a) air (b) aluminum doped.

3.2 Resistance Measurements

The thin film resistivity greatly influenced by the interaction of the conduction electrons with the surface. In other words, it is a measure of the material's inherent surface resistance to current flow. The grain size and resistance of ZnO thin films measured at room temperature is given in table-1. Fig. 4 shows that as the grain size increases the resistances of the film decreases linearly (i.e. resistance is inversely proportional to the grain size). One of the reasons for this is the decrease in grain boundary when the grain size increases. The electrical resistance in aluminium doped sample is much less than that of pure sample, due to the contribution from *Al* ions on the substitutional site of Zn ions and *Al*- interstitial atoms.

Table 1. Orientation index (*O. I.*), Grain Size, Resistance (*R*), Band Gap E_g of different samples

Sl. No.	Sample details	O. I.	Grain Size(nm)	R (K Ω)	E_g (eV)
1	Annealed in oxygen atmosphere	1.17	18	11	3.32
2	Annealed in air	1.23	21.35	9	3.30
3	Annealed in argon atmosphere	1.47	25.8	6	3.21
4	Annealed in nitrogen atmosphere	1.70	29.15	4	3.11
5	Aluminium doped annealed in air	2.08	33.35	1.45	3.08

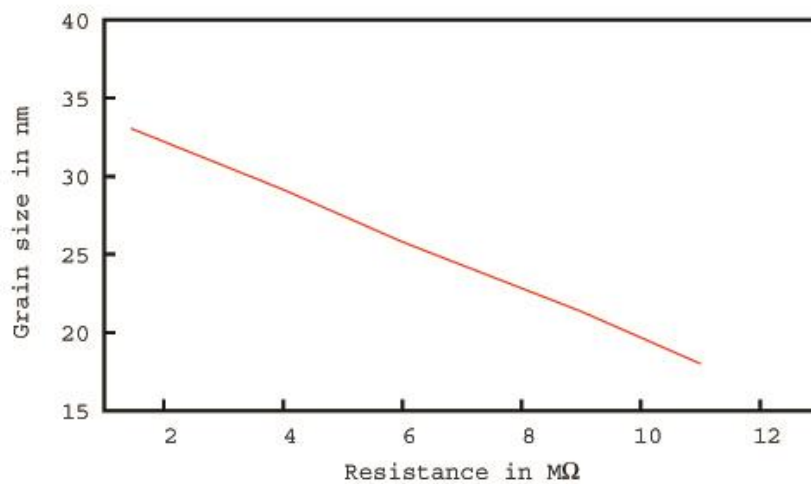


Fig. 4. The plot of Grain size vs Resistance of different samples.

3.3 Optical properties of ZnO Films

The fig. 5 shows the optical absorbance spectrum of ZnO thin film (annealed at 450°C in air for half an hour) using UV-visible region from 200 - 800 nm. The figure 5 (inset) depicts the plot of $(\alpha hv)^2$ vs energy, hv . The band gap of the samples is estimated by extrapolation of the linear relationship between $(\alpha hv)^2$ and hv , according to the equation $hv = A (hv - E_g)^{1/2}$, where α is the absorption coefficient, hv is the photon energy, E_g is the optical band gap and A is a constant. The values of direct band gap (E_g) are calculated from the intercept of $(\alpha hv)^2$ vs hv curve. The band gap value of pure ZnO thin film is found to be 3.30 eV which is slightly smaller than the reported value (3.37 eV). This is because the values of band gap E_g depend on many factors like the nature and concentration of precursors, the structural defects and the crystal structure of the films etc. It is also reported that the band gap difference between the samples is due to the grain boundaries and imperfections of the polycrystalline thin films [20]. Band gap is calculated for the samples annealed in oxygen atmosphere, in air, argon atmosphere, and nitrogen atmosphere and doped with aluminium. The values are given in table-1. The plot of grain size vs band gap of different samples is shown in the fig. 6. Table-1 and fig.6 show that band gap decreases with increase in grain size of the film.

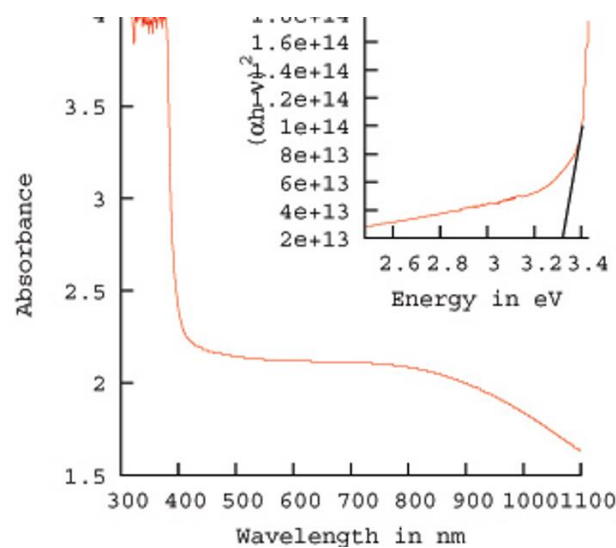


Fig. 5. Absorbance for the sample annealed in air. The inset indicates optical band gap energy of the sample.

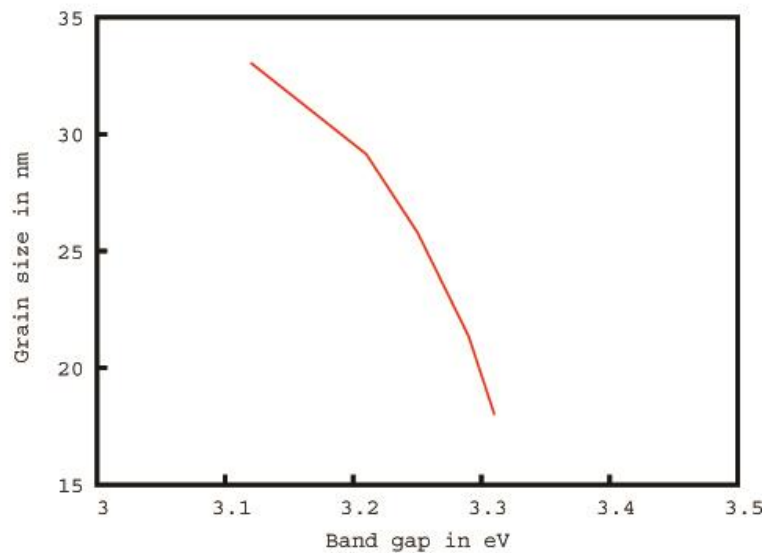


Fig. 6. The plot of Grain size vs optical band gap energy of different samples.

3.31 Photoconductivity Studies

The photoconductivity is a phenomenon in which samples become electrically conductive due to the absorption of electro-magnetic radiation. When light is absorbed by samples, the number of free electrons and holes changes and raises its electrical conductivity [21]. The photo current and dark current of samples annealed in atmospheres of oxygen (A), air (B), argon (C), nitrogen (D) are shown in fig. 7 and aluminium doped sample is shown in the fig. 8. From the figures it is clear that both the dark and photo current of the samples increase linearly with applied field. For the same applied field, the photo current is greater than dark current which reveals the positive photo-conducting behaviour of sample. In the case of nitrogen annealed sample sample (D) photo current and dark current is found to be more compared to samples annealed in oxygen (A), air (B), argon (C). In case of the aluminium doped sample photo current and dark current is more than the samples annealed in atmospheres of oxygen (A), air (B), argon (C), nitrogen (D). This infers that samples annealed in atmospheres of nitrogen (D) aluminium doped samples were able to generate more photo current than the other samples. This makes them promising candidate for Solar Cells. The results also indicate that the ZnO is beneficial to photodynamic therapy technology [22].

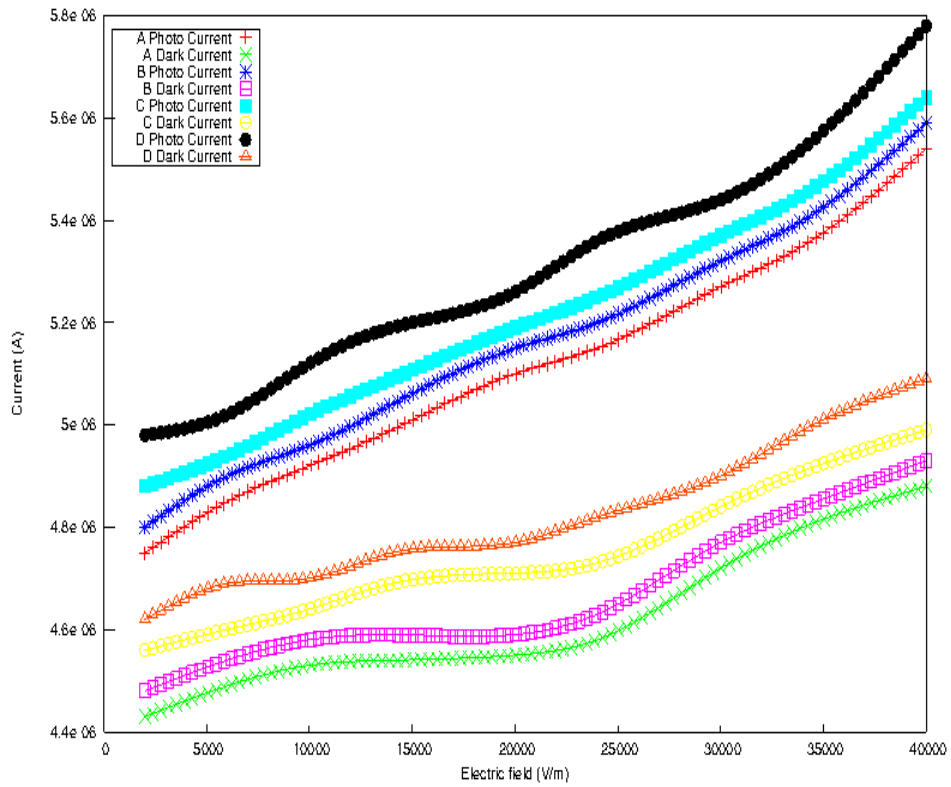


Fig. 7. The photoconductivity of the samples annealed in (A) oxygen atmosphere (B) air (C) argon atmosphere (D) nitrogen atmosphere.

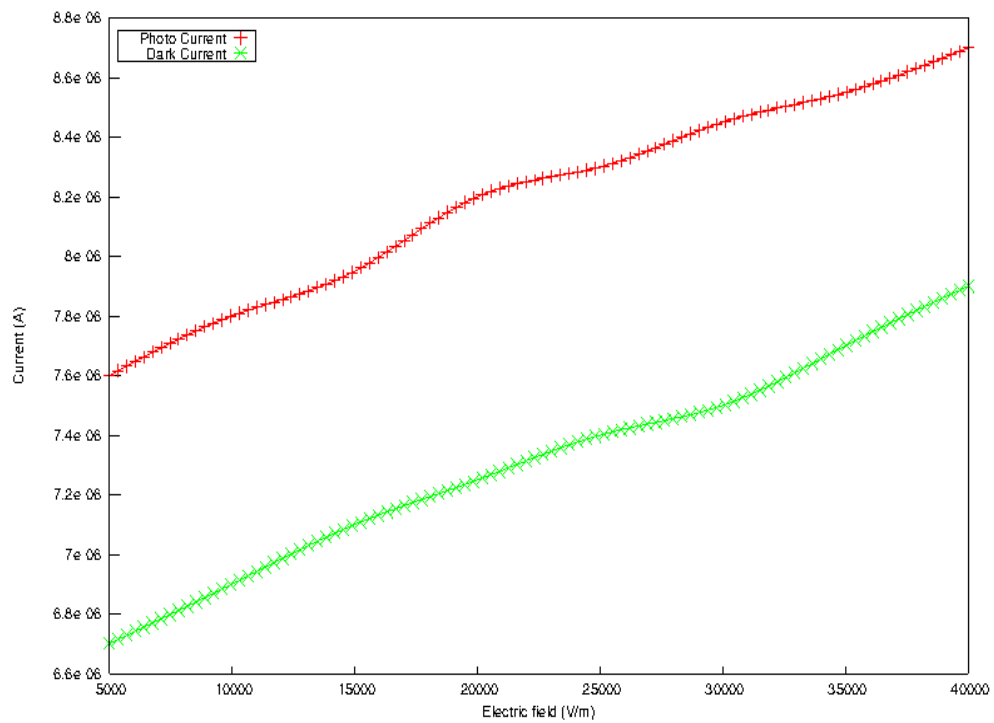


Fig. 8. Photoconductivity pattern of the aluminium doped sample.

3.4 Elemental analysis by EDAX

Energy-dispersive X-ray spectroscopy (EDAX) is an analytical technique used for the elemental analysis or chemical characterization of a sample. Theoretically expected stoichiometric mass% of Zn and oxygen are 80.3 and 19.7. Table -2 gives atomic percentage of oxygen and Zn in the samples obtained from the EDAX studies. From table- 1 and 2 it is clear that as the orientation index increases, the oxygen content of the samples decreases. This means that, oxygen vacancy is more in samples that has more oriented grain growth.

Table 2. Atomic% of oxygen and zinc in different samples

Sl. No.	Sample details	Atomic% of oxygen	Atomic% of zinc
1	Annealed in oxygen atmosphere	35.86	64.14
2	Annealed in air	27.34	72.66
3	Annealed in argon atmosphere	26.23	73.77
4	Annealed in nitrogen atmosphere	25.87	74.13
5	Aluminium doped annealed in air	23.46	76.54

Native or intrinsic defects are imperfections in the crystal lattice. They include vacancies (missing atoms at regular lattice positions), interstitials (extra atoms occupying interstices in the lattice) and anti sites (a Zn atom occupying an O lattice site or vice versa) [23, 24]. ZnO thin films annealed in air, argon and nitrogen atmosphere are in an oxygen deficient environment which results in oxygen vacancies or zinc vacancies. It is reported that Al- doping will create oxygen vacancies due to the substitution of Zn by Al^[6]. This confirms that, oxygen vacancy creation is the mechanism behind the enhanced oriented grain growth. When sample synthesized in oxygen rich environment, the oxygen content is more and oriented grain growth is less compared to other samples. Data from table-1 and 2 agree with this.

4. Conclusions

From the studies following conclusions can be drawn. Oriented grain growth in ZnO thin films increases in the order of samples annealed in atmospheres of oxygen, air, argon, nitrogen and aluminium doped. As the oriented grain growth increases the needle like structure disappears and flowered structure becomes prominent. When the oriented grain growth increases, crystallinity of the thin film improves, photo current and dark current increases, resistance and band gap decreases. ZnO thin films having good crystallinity with preferential (002) orientation is a prerequisite for the fabrication of devices like UV diode lasers, acousto-optic devices etc. A possible mechanism for the oriented grain growth was also investigated. From energy dispersive X-ray analysis, it is inferred that oxygen vacancy creation is responsible for the enhanced oriented grain growth in ZnO thin films by annealing the samples in air, in atmospheres of argon, nitrogen and aluminium doping.

Acknowledgements

The authors are thankful for financial support from University Grants Commission, Government of India through a research grant (MRP(S) - 986/ 10 - 11/ KLMG027/ UGC - SWRO).

References

- [1] G. Xiangdong, L. Xiaomin, Y. Weidong, *J. of Wuhan University of Technology Materials Science Edition*. **20**, 23 (2005) .
- [2] D. Fang, C. Li, N. Wang, P. Li and P. Yao, *Cryst. Res. Technol.* **48**(5), 265 (2013).
- [3] V. Shelke, B. Sonawane, M. Bhole, D. Patil. *J. of Materials Science Materials in Electronics*. **23**, 451(2012).
- [4] T. Yen, D. Strome, S. J. Kim, A. Cartwright, W. A Anderson, *J. of Electronic Materials*. **37**, 764 (2008).
- [5] J. H. Park, H. K. Pak, C. R. Cho, *J. of the Korean Physical Society*. **49**(1), S584 (2006).
- [6] R. Chandramohan, V. Dhanasekaran, S. Ezhilvizhian, T. Vijayan, J. Thirumalai, A. Peter, T. Mahalingam. *J. of Materials Science Materials in Electronics*. **23**, 390 (2012).
- [7] J. Son, J. Shim, N. Cho, *J. Of Metals and Materials International*. **17**, 99 (2011)
- [8] P. Murmu, J. Kennedy, B. Ruck, G. Williams, A. Markwitz, S. Rubanov, A. Suvorova, *J. of Materials Science* **47**, 1119 (2012).
- [9] H. Zhu, J. Hpkes, E. Bunte, A. Gerber, S. Huang, *Thin Solid Films*. **518**(17), 4997 (2012).
- [10] W. H. Luo, T. K. Tsai, J. C. Yang, W. M. Hsieh, C. H. Hsu, J. S. Fang, *J. of Electronic Materials*. **38**, 2264 (2009).
- [11] Y. Kokubun, H. Kimura, S. Nakagomi, *Japanese J. of Appl. Phys.* **42**(Part 2, No. 8A), L904 (2003).
- [12] Y. Lee, H. Kim, Y. Roh. *Japanese J. of App. Phys.* **40**(Part 1, No. 4A), 2423 (2001).
- [13] Pathan, H., Lokhande, C. *Bulletin of Materials Science*. **27** (2004).
- [14] B. R. Sankapal, R.S. Mane, C. D. Lokhande. *J. of Materials Science Letters*. **18**, 1453 (1999).
- [15] S. R. Jian, H. G. Chen, G. J. Chen, J. S. Jang, J. Y. Juang, *Current Appl. Phys.* **12**(3), 849 (2012).
- [16] F. Li, L. Bo, S. Ma, X. Huang, L. Ma, J. Liu, X. Zhang, F. Yang, Q. Zhao, *Superlattices and Microstructures*. **51**(3), 332 (2012).
- [17] J. Wang, V. Sallet, F. Jomard, A. M. Rego, E. Elamurugu, R. Martins, E. Fortunato, *J. Of Thin Solid Films* **515**(24), 8780 (2007).
- [18] M. Ristov, G. Sinadinovski, M. Mitreski, *J. Thin Solid Films*. **167**(12) (1988).
- [19] S. Cho, *Transactions on Electrical and Electronic Materials*,. **10**(6), 185 (2009)
- [20] M. Saleem, L. Fang, A. Wakeel, M. Rashad, C. Y. Kong, *World Journal of Condensed Matter Physics*. **2**(6), 10 (2012)
- [21] M. H. Huang, S. Mao, H. Feick, *Science*, vol. 292, no. 5523, pp. 1897–1899 (2001).
- [22] S. John, S. Marpu, J. Li, M. Omary, Z. Hu, Y. Fujita, A. Neogi, *J. Nanosci Nanotechnol.* **10**(3), 1707-12 (2010).
- [23] S. E Harrison, *Phys. Rev.* **93**, 52 (2004).
- [24] D. G Thomas, *Phys. Chem. Solids (USA)*. **3**, 229 (1957).